Research Square

Preprints are preliminary reports that have not undergone peer review.
They should not be considered conclusive, used to inform clinical practice,
or referenced by the media as validated information.

Classification of Primary and Secondary Response Genes in A549 Cells to Short-term Manganese Exposure: Bioinformatic Analysis and Experimental Verification

Xinyu Liu
Beihang University
Yishan Jin
Beihang University
Shuiqing Yang
Beihang University
Huizhi Xiang
Beihang University
Chunhong Yu
chunhongyu@buaa.edu.cn
Beihang University
Zongchun Yi
Beihang University

Research Article

Keywords: manganese, early response gene, primary response genes, secondary response genes, transcriptomic, A549 cells

Posted Date: November 17th, 2026

DOI: https://doi.org/10.21203/rs.3.rs-11639813/v1

License: This work is licensed under a Creative Commons Attribution 4.0 International License.
Read Full License

Additional Declarations: No competing interests reported.

Classification of Primary and Secondary Response Genes in A549 Cells to Short-term Manganese Exposure: Bioinformatic Analysis and Experimental Verification

Xinyu Liu[1,#], Yishan Jin [2,3,#], Shuiqing Yang[2,4,#], Huizhi Xiang[1] , Chunhong Yu[1,*] and Zongchun Yi[2,*]

[1] School of Engineering Medicine, Beihang University, Beijing 100191, China

[2] School of Biological Science and Medical Engineering, Beihang University, Beijing 100191, China

[3] Chinese Academy of Medical Science & Peking Union Medical College, Beijing 100730, China

[4] Department of Rehabilitation, Beijing Rehabilitation Hospital, Capital Medical University, Beijing 100043, China

[#] These authors contributed equally to this work.

[*]Corresponding authors

Chunhong Yu, School of Engineering Medicine, Beihang University, 37 Xueyuan Road, Beijing 100191, China. E-mail: chunhongyu@buaa.edu.cn. Zongchun Yi, School of Biological Science and Medical Engineering, Beihang University, 37 Xueyuan Road, Beijing 100191, China. Fax: +86 10 8231 5554. E-mail address: yizc@buaa.edu.cn.

Funding

This work was supported by the National Natural Science Foundation of China (Grant No. 81573192), the Scientific and Technological Innovation Project of China Academy of Chinese Medical Sciences (Grant No. CI2023C020YL), and the Fundamental Research Funds for the Central Universities (Grant No. JK2024-2-07).

Abstract

Background

Although manganese (Mn) is an essential trace element, excessive exposure has been associated with adverse effects on the respiratory, nervous, and reproductive systems. Many studies of Mn toxicity have focused on downstream cellular injury, leaving the immediate transcriptional responses to exposure less well characterized. We therefore investigated early response genes induced by short-term Mn exposure in human A549 lung adenocarcinoma cells.

Methods

A549 cells were exposed to $MnCl_2$ for 4 h, and 300 μM was selected for RNA sequencing. To distinguish responses that persist during protein synthesis inhibition from cycloheximide (CHX)-sensitive responses, a subset of cells received 50 μM CHX for 30 min before Mn exposure. Selected genes were assessed by reverse transcription PCR across exposure times and Mn concentrations. Gene Ontology, KEGG, and protein–protein interaction analyses were performed.

Results

Exposure to 300 μM $MnCl_2$ for 4 h upregulated 297 genes. Comparison with CHX-pretreated cells identified 92 putative primary response genes, including *FOS*, *JUN*, *JUNB*, *EGR1*, and *PTGS2*, and 119 putative secondary response genes, including *HMOX1*, *SQLE*, *MSMO1*, *DHCR7*, and *TGFB1*. Enrichment analyses implicated responses to oxygen levels and metabolic processes, including the HIF-1 signaling pathway. Reverse transcription PCR supported the expression patterns of selected genes.

Conclusion

Short-term Mn exposure elicits distinct early transcriptional responses in A549 cells. The identified genes and enriched pathways provide candidates for further investigation of Mn toxicity.

Keywords: manganese; early response gene; primary response genes; secondary response genes; transcriptomic; A549 cells

Introduction

Manganese (Mn) is an essential trace element that plays a critical role in maintaining normal development and physiological functions in living organisms. Due to its redox activity, Mn commonly exists in various oxidation states (+2, +3, +4, +6, and +7), typically occurring as oxides, silicates, or carbonates in the environment. In biological systems, Mn^{2+} represents the most stable and predominant form, whereas Mn^{3+} acts as a potent oxidant that tends to disproportionate into Mn^{2+} and Mn^{4+} or forms stable complexes with proteins [1], Mn is absorbed through ingestion, inhalation, and dermal permeation; it is rapidly absorbed via the gastrointestinal tract and lungs before being distributed to different tissues through systemic circulation [2].

Exposure to high levels of Mn tends to accumulate in the brain, liver, kidney, bone and pancreas, resulting in Mn intoxication. Mn exposure arises from diverse sources, including contaminated drinking water, soil, air pollution, and industrial activities such as the production of batteries, steel, and ceramics [3]. Although regulatory bodies like the American Conference of Governmental Industrial Hygienists Threshold Limit Value (ACGIH TLV) and the Japan Society for Occupational Health (JSOH) have set stringent air concentration limits (0.1 mg/m^3 for total dust and 0.05 mg/m^3 for respirable dust), Mn tends to accumulate significantly in the human body even under these guidelines [4]. Notably, elevated blood Mn concentrations exceeding 0.013 mg/dm^3 have been linked to central nervous system dysfunction, indicating that Mn-mediated toxicity is driven more by systemic cellular accumulation than by external exposure metrics alone [5].

Mn poisoning can manifest in various health issues including Parkinson's disease, liver impairments, hepatic cirrhosis, polycythemia, hypermangnesemia, and dystonia along with damage to the respiratory, nervous or reproductive system [6]. Extensive research has shown that Mn toxicity can be regulated by

oxidative stress, mitochondrial dysfunction, endoplasmic reticulum stress, apoptosis, autophagy, protein misfolding, and other metal homeostasis disruption [2]. Epidemiological studies have demonstrated that prolonged or excessive exposure to Mn can adversely affect human lung function. Furthermore, residents living in proximity to areas with Mn emissions exhibit a higher incidence and mortality rate of pneumonia [7]. Vulnerable populations, including young children, may experience detrimental effects on lung function even when exposed to minimal levels of Mn [8]. However, the immediate-early molecular mechanisms driving the onset of Mn toxicity remain incompletely understood. Notably, the majority of existing studies have predominantly focused on late-stage pathological manifestations or downstream cascades (e.g., oxidative stress, mitochondrial damage, and apoptosis), whereas the transcriptional regulatory networks activated within the first few hours of Mn exposure remain poorly characterized. Consequently, there is a critical need to systematically investigate the early-onset molecular events that initiate Mn-induced cellular stress.

A specific group of genes responds transiently and rapidly to external stimuli like physiological and pathological factors, innate and adaptive immune responses, or cellular stress across various cell types [9,10]. These genes are classified into two stages: the rapid protein synthesis-independent induction of primary response genes (PRGs), also known as immediate-early genes (IEGs); and the subsequent protein synthesis-dependent induction of secondary response genes (SRGs) [11,12]. PRGs can encode for a wide range of cytoplasmic enzymes, secreted proteins, and transcription factors. Approximately 20% of known PRGs are transcription factors like *FOS*, *FOSB*, *FOSL1*, *JUN*, *JUNB,* and early growth response protein (*EGR1–EGR4*). Activation of PRGs can regulate acute inflammation, neuronal activity,and cell proliferation and differentiation [13,14,15]. Abnormal expression of PRGs is implicated in malignant transformation within cells and has been observed across various cancer types [12,13]. While

cells show various biological responses under different external stimuli including neuronal survival and plasticity, cardiac stress response, immune response and oncogenetic transformation, which are closely related to the different responses of PRGs [16,17,18]. However, the specific role of Mn-induced early response genes in cellular cytotoxicity remains largely undefined. To address this gap, the present study specifically focuses on the molecular mechanisms underlying short-term Mn exposure-induced early response genes, aiming to elucidate the primary transcriptional programs triggered at the initial phase of Mn toxicity.

In this study, human lung epithelial (A549) cells were utilized as an established and widely validated *in vitro* model for respiratory toxicology and metal inhalation research [19,20]. To distinguish between PRGs and SRGs, we employed cycloheximide (CHX), a glutarimide antibiotic that inhibits eukaryotic protein synthesis by blocking mRNA translation [21]. Early response genes can be transcribed within minutes without the necessity of de novo protein synthesis [10,22]. Mn is an essential trace element, with physiological serum levels in healthy populations ranging from 0.19 to 3.33 μg/L (approximately 0.0035 to 0.061 μM) [23]. However, in occupational exposure scenarios (e.g., welders or miners), localized concentrations in lung tissue or olfactory epithelium can drastically exceed systemic serum levels. Therefore, in vitro inhalation toxicology studies frequently employ higher concentrations to elicit measurable and robust stress responses. Based on preliminary screening (0–1200 μM), we selected 300 μM as the optimal sub-lethal dose to robustly initiate the acute transcriptional program without causing immediate, overwhelming cell death.

By combining genome-wide RNA sequencing (RNA-seq) with targeted experimental validation, we systematically investigated the changes in A549 cells under short-term Mn exposure and the modulatory effects of cycloheximide (CHX). Mn-induced early response genes were identified and classified into

PRGs and SRGs, followed by protein-protein interaction (PPI) network construction and GO/KEGG enrichment analyses. This integrative approach aims to bridge the gap between systemic exposure ~~data~~ and early cellular mechanisms, uncovering the molecular pathways—particularly oxygen sensing and HIF-1 signaling—that drive the onset of Mn-induced toxicity.

Materials and methods

Cell culture and treatment

Human lung adenocarcinoma A549 cells were obtained from American Type Culture Collection and maintained in RPMI-1640 culture medium (Invitrogen) supplemented with 10% (V/V) fetal bovine serum (FBS) (HyClone), 100 U/mL penicillin (Sigma-Aldrich) and 100 μg/mL streptomycin (Sigma-Aldrich) in a humidified 5% carbon dioxide (CO_2) incubator at 37°C. After A549 cells were seeded in a 6-well plate for 12 h, the cells were treated with 300 μM $MnCl_2$ for 4 h and protein synthesis inhibitor, 50 μM CHX (Sigma-Aldrich) were pretreated for 30 min before $MnCl_2$ treatment.

Cell morphology analysis

Exponentially growing A549 cells were digested with trypsin (SigmaAldrich, USA) (in PBS containing 0.02% EDTA) for 5 min at 37°C, then 20% fetal bovine serum was added to stop the digestion, and cells were collected by centrifugation at 800 ×g for 5 min and re-suspended in fresh culture medium. To visually assess the acute cellular stress response and to confirm the sub-lethal nature of the chosen dose, A549 cells were treated with a gradient of 0–500 μM $MnCl_2$ (Sigma-Aldrich) for 4–24 h. Cell morphology was photographed by phase contrast microscope (ELWDN.A.0.30). The total number of typical epithelial-like cells (fully spread and adherent) versus cobblestone-like cells (rounded, contracted cells indicating cytoskeletal stress) were counted using a hemocytometer.

Reverse transcription-polymerase chain reaction (RT-PCR)

After A549 cells were seeded in a 6-well plate for 12 h, the cells were treated with 300 μM $MnCl_2$ for 4 h and 50 μM CHX were pretreated for 30 min before $MnCl_2$ treatment. Total RNA was extracted with RibozolTM RNA Extraction Reagent (Amresco). RNA was converted to cDNA using the RevertAid™ First Strand cDNA Synthesis Kit (Fermentas). The PCR amplification reaction was performed in a 10 μL reaction volume containing 2 μL cDNA, 5 μL PCR mix (2×GoldStar Best MasterMix, Cwbiotech), 0.5 μL forward primer (10 μM), 0.5 μL reverse primer (10 μM) and 2 μL ddH2O in a Tgradient Thermocycler (Biometra). The reactions were proceeded under the following conditions: (1) an initial step at 95°C for 10 min; (2) 30–35 cycles of denaturation at 94°C for 30 s, annealing at 52–60°C for 30 s and extension at 72°C for 60 s; (3) terminate the reaction at 72°C for 5 min. The PCR primer sequences are listed in Table 1. *β-actin* was used as an internal control. The amplified DNA products were electrophoresed on a 2% agarose gel with ethidium bromide. The DNA bands were visualized and photographed with ImageMaster Video Documentation System (Pharmacia Biotech).

Table 1. Sequences of primers used in reverse transcriptase PCR

Gene	Sequence of primers (5'- 3')	Size(bp)
FOS	F- AGTGCCAACTTCATTCCCAC	265
	R- CCCTTCGGATTCTCCTTTTC	
FOSB	F- CGAGAGGAGACGGAGACAGA	139
	R- CTTCGTAGGGGATCTTGCAG	
FOSL1	F- TCTTCACCTACCCCAGCACTC	220
	R- GCTGGAGTTGGATGTGGGATAC	
FOSL2	F- CAGCATTGCTGGGGGCTTCTA	196
	R- TGATTGGTCCCCGCTGCTACT	
JUN	F- CCCCAAGATCCTGAAACAGA	168
	R- CCGTTGCTGGACTGGATTAT	
JUNB	F- GCCTCCGGGACAGTACTTTTA	148
	R- CGTCACGTGGTTCATCTTG	
JUND	F- CGTTGGTTGTGTGTGTGTGTG	175
	R- CAGGAATGTGGACTCGTAGCA	

EGR1	F- TGACCGCAGAGTCTTTTCCT	203
	R- TGGGTTGGTCATGCTCACTA	
PTGS2	F- CCTGAGCATCTACGGTTTGC	145
	R- ACTGCTCATCACCCCATTCA	
SOD2	F- GCAGTGTGCGGCACCAGCAG	216
	R- TCCCTTGGCCAACGCCTCCT	
HMOX1	F- AGCATGTCCCAGGATTTGTC	144
	R- GTACAAGGAGGCCATCACCA	
ITGA5	F- GGCTTCAACTTAGACGCGGAG	140
	R- TGGCTGGTATTAGCCTTGGGT	
BHLHE40	F- AGCAGTGGTTCTTGAACTTACC	237
	R- ACAAGCTGCGAAGACTTCAGG	
VEGFA	F- TTGCCTTGCTGCTCTACCTCCA	126
	R- GATGGCAGTAGCTGCGCTGATA	
CDKN1A	F- TGTCCGTCAGAACCCATGC	139
	R- AAAGTCGAAGTTCCATCGCTC	
KDM3A	F- GTGCTCACGCTCGGAGAAA	156
	R- GTGGGAAACAGCTCGAATGGT	
ARRDC3	F- ATGCAAGAGGACATGCGAAAG	161
	R- GTGGAAGCCTTCTTCGGAATTAT	
IL11	F- CGAGCGGACCTACTGTCCTA	272
	R- GCCCAGTCAAGTGTCAGGTG	
SQLE	F- TGACAATTCTCATCTGAGGTCCA	179
	R- CAGGGATACCCTTTAGCAGTTTT	
MSMO1	F- TGCTTTGGTTGTGCAGTCATT	143
	R- GGATGTGCATATTCAGCTTCCA	
DHCR7	F- GCTGCAAAATCGCAACCCAA	123
	R- GCTCGCCAGTGAAAACCAGT	
TGFB1	F- GGCCAGATCCTGTCCAAGC	201
	R- GTGGGTTTCCACCATTAGCAC	
SEMA4B	F- GAGCGGCCATTCCTCAGATTC	91
	R- CACCCACGTACAGGGTCCT	
β-actin	F-TGGACTTCGAGCAAGAGATGG	289
	R- ATCTCCTTCTGCATCCTGTCG	

High-throughput Transcriptome analysis (RNA-seq)

The genome-wide transcriptome analysis was analyzed as described previously [24]. Differentially expressed genes (DEGs) analysis was indicated with the absolute log (fold change of Mn/C) values and the adjusted P-value <0.05 was considered differentially expressed. The volcano plot of DEGs was

performed by R language. Gene Ontology (GO) enrichment analysis of DEGs was conducted by over-representation analysis (ORA) using the online database WebGestalt (http://www.webgestalt.org) [25]. The GO homepage was utilized to enhance the molecular functions, cellular components, and biological processes associated with differential genes. The histogram was generated using the R language, displaying the names of the top 30 items with the highest enrichment degree and the respective number of genes contained in each item. The DEGs of the KEGG signaling pathway was analyzed through both the DAVID homepage and KEGG homepage enrichment. A bubble diagram was created using R language, presenting the names of the 20 items with their corresponding enrichment degree, enrichment factor, number of genes contained, and the P value. The HIF-1 signaling pathway was conducted using the KEGG database (http://www.kegg.jp) [26]. The protein-protein-interaction network was constructed using STRING (http://string-db.org).

Statistical analysis

Experimental data from at least three independent biological replicates ($n \geq 3$) were expressed as the mean ± standard deviation (SD). The statistical analyses were performed using either the Student's test or a two-way ANOVA followed by the GraphPad Prism 8 (GraphPad Software, CA, USA). Results at $p < 0.05$ or less were considered statistically significant.

Results

Dose-dependent effects of $MnCl_2$ on A549 cell morphology

After A549 cells (1×10^5 cell/ml) were seeded in a 24-well plate for 12 h, the cells were treated with 0–500 μM $MnCl_2$ for 4 h and 24 h, respectively. Cell morphology analysis showed that the percentage of epithelial-like cells decreased in a concentration-dependent manner after exposure to 0, 100, 200, 300,

400 and 500 μM $MnCl_2$ for 4 h, which were 76.8%, 71.3%, 62.4%, 59.4%,57.2% and 52.6%, respectively (Fig.1a). Likewise, the percentage of epithelial-like cells ranged from 85.7% to 31.8% when exposed to 0–500 μM $MnCl_2$ for 24 h (Fig.1b). Conversely, the population of cobblestone-like cells —characterized by a rounded, contracted morphology indicative of cytoskeletal stress—increased in a concentration-dependent manner at both time points. Notably, these cobblestone-like cells remained predominantly negative for trypan blue staining, suggesting they were highly viable and membrane-intact despite the morphological shift, indicating a robust physiological stress response rather than widespread necrosis. Consequently, 300 μM $MnCl_2$ was selected as the optimal sub-lethal concentration for the subsequent time-course evaluations.

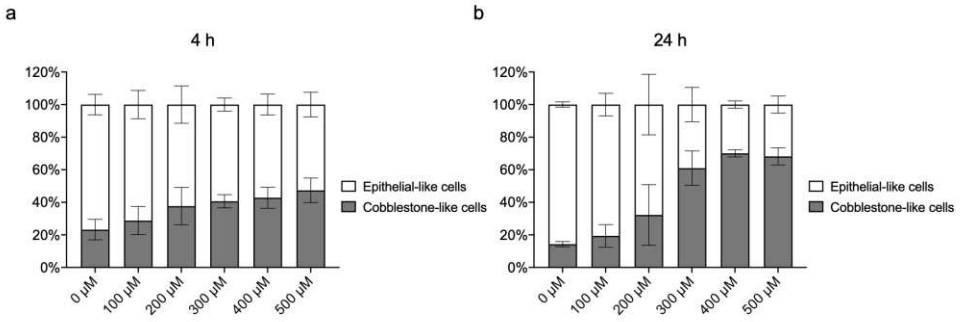


Fig. 1 The effects of $MnCl_2$ on cell morphology in A549 cells. A549 cells were treated with 0–500 μM $MnCl_2$ for 4 h (a) and 24 h (b), respectively. Percentages of epithelial-like cells and cobblestone-like cells were counted using a haemocytometer. The value was shown as mean ± SD, n = 3.

Time-course expression of classical early response genes in A549 cells following Mn exposure

To evaluate the temporal dynamics of gene expression, A549 cells were treated with 300 μM $MnCl_2$ for

1, 2, 3, and 4 h. The mRNA levels of classic early response genes (ERGs), including *FOS, FOSB, FOSL1, FOSL2, JUN, JUNB, JUND, EGR1, SOD2, PTGS2,* and *HMOX1*, were measured by RT-PCR (Fig. 2a-l).

The FOS family of transcription factors includes *FOS*, *FOSB*, *FOSL1*, and *FOSL2*, as well as smaller *FOSB* splice variants [27]. The mRNA expression of *FOS* considerably increased to 1.2, 1.4 and 1.5 times of the control A549 cells when treated with Mn for 2 h, 3 h and 4 h, respectively (Fig.2b). The mRNA expression of *FOSB* considerably increased to more than twice the control level after 3 h and 4 h of Mn exposure (Fig.2c). The mRNA expression of *FOS* and *FOSB* increased in time-dependent manners whereas the mRNA expression of *FOSL1* and *FOSL2* showed no crucial change (Fig.2d-e).

The Jun family members (JUN, JUNB and JUND) can homodimerize and heterodimerize with FOS members [28]. When treated with Mn for 1 h, 2 h, 3 h and 4 h, the mRNA expression of *JUN* increased in a time-dependent manner and considerably upregulated to 1.3 times of the control A549 cells when treated with Mn for 3 h; the mRNA expression of *JUNB* considerably increased to 1.2, 1.3 and 1.2 times of the control A549 cells when treated with Mn for 2 h, 3 h and 4 h, respectively (Fig.2f-g). However, the mRNA expression of *JUND* showed no crucial change (Fig.2h).

In addition, the mRNA expression of *EGR1* and *PTGS2* increased in time-dependent manners, peaking at 5.3 and 2.2 times of the control A549 cells when treated with Mn for 4 h, respectively. When treated with Mn for 1 h, 2 h, 3 h and 4 h, the mRNA expression of *SOD2* and *HMOX1* showed no obvious change except *HMOX1* increased slightly to 1.1 times of the control cells when treated for 4 h (Fig.2i-l). When treated with Mn for 4 h, the mRNA expression of these early response genes showed similar trends in the transcriptomic assay and RT-PCR analysis, which further supported the up-regulated mRNA expression of *FOS*, *FOSB*, *JUN*, *JUNB*, *EGR1*, *PTGS2* and *HMOX1* (Fig.2m). The gene clustering

analysis showed that *JUN* and *FOS* were clustered together, whereas *PTGS2* and *FOSB* were clustered together (Fig.2n). The JUN and FOS family members form the group of AP-1 proteins, which bind to TPA-responsive elements (TRE's; TGAC/GTCA) in the target genes after dimerization, are important nuclear transcription factors that respond to stimulus.

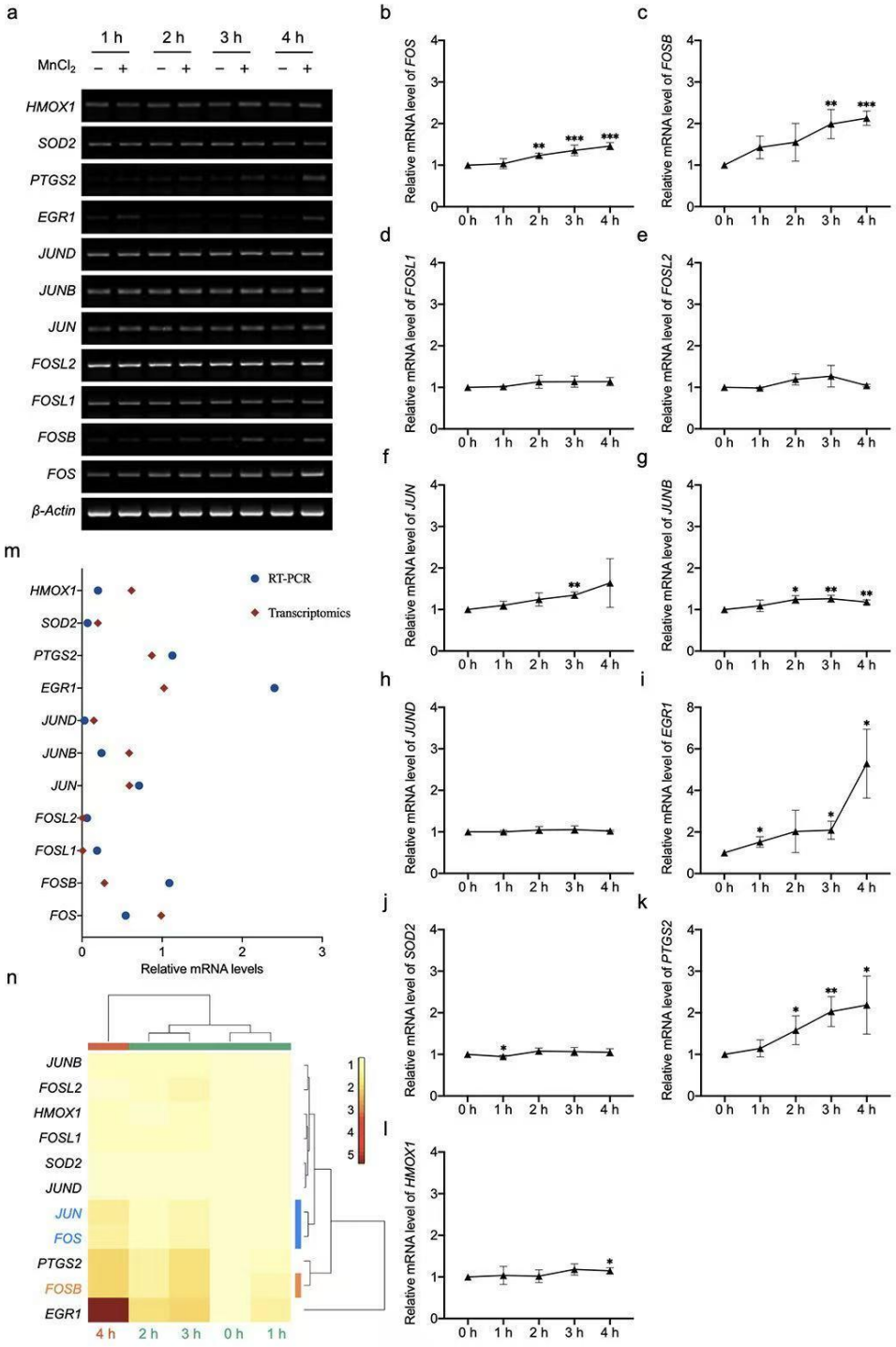


Fig. 2 The Mn-induced early response genes expression in A549 cells. The A549 cells were treated with 300 μM $MnCl_2$ for 1 h, 2 h, 3 h and 4 h. (a-l) The mRNA expression of early response genes was estimated by RT-PCR. (m) The comparative analysis of Mn-induced early response genes expression by RT-PCR

and transcriptomic assay. (n) The clustering analysis of the mRNA expression of early response genes. The value was shown as mean ± SD, n = 3. Statistical significance was determined by a two-tailed paired Student's t test. *P < 0.05, **P < 0.01 and ***P < 0.005 (vs corresponding "0 h" group)

The transcriptomic landscape and classification of Mn-induced PRGs and SRGs in A549 cells

To distinguish between direct and indirect transcriptional responses, A549 cells were pretreated with the protein synthesis inhibitor CHX (50 μM) before exposure to 300 μM $MnCl_2$ for 4 h. Transcriptomic profiling identified 878 differentially expressed genes (DEGs) induced by Mn, consisting of 297 upregulated and 581 downregulated genes (Fig.3a). In the presence of Mn, CHX pretreatment induced differential expression in 8,532 genes (4,467 upregulated and 4,065 downregulated) relative to cells treated with Mn alone (Fig.3b). Notably, CHX pretreatment modulated the expression of 540 specific Mn-induced DEGs (Fig.3c).

To investigate the early response genes after Mn exposure, we focused on the upregulated DEGs. Among the 297 upregulated DEGs after Mn exposure, 92 DEGs including *JUN*, *JUNB*, *BHLHE40* and *ITGA5*, were upregulated when pre-treated with CHX. The levels of these genes were not inhibited by protein synthesis inhibitors and they could be classified as the primary response genes (PRGs) (Supplementary Table 1). On the other hand, 119 DEGs like *SEMA4B*, *SQLE*, *TGFB1*, and *MSMO1*, were downregulated when pre-treated with CHX. The levels of these genes were inhibited by protein synthesis inhibitor and they could be classified as the secondary response genes (SRGs) (Fig.3d) (Supplementary Table 2).

The protein interaction network of Mn-induced PRGs and SRGs was classified into seven main clusters using STRING database (Fig.3e). Cytohubba's MCC algorithm was used to find the hub nodes

with high connectivity with others in the network. As a result, proteins encoded by 9 PRGs (*CDKN1A*, *PTGS2*, *JUN*, *FOS*, *EGR1*, *CXCR4*, *SOX9*, *BMP2*, *HMGCS1*) and 11 SRGs (*MVK*, *DHCR7*, *MSMO1*, *NSDHL*, *CYP51A1*, *FDFT1*, *SQLE*, *HSPA5*, *HMOX1*, *TGFB1*, and *NOTCH1*) were determined as the hub proteins (Fig.3f).

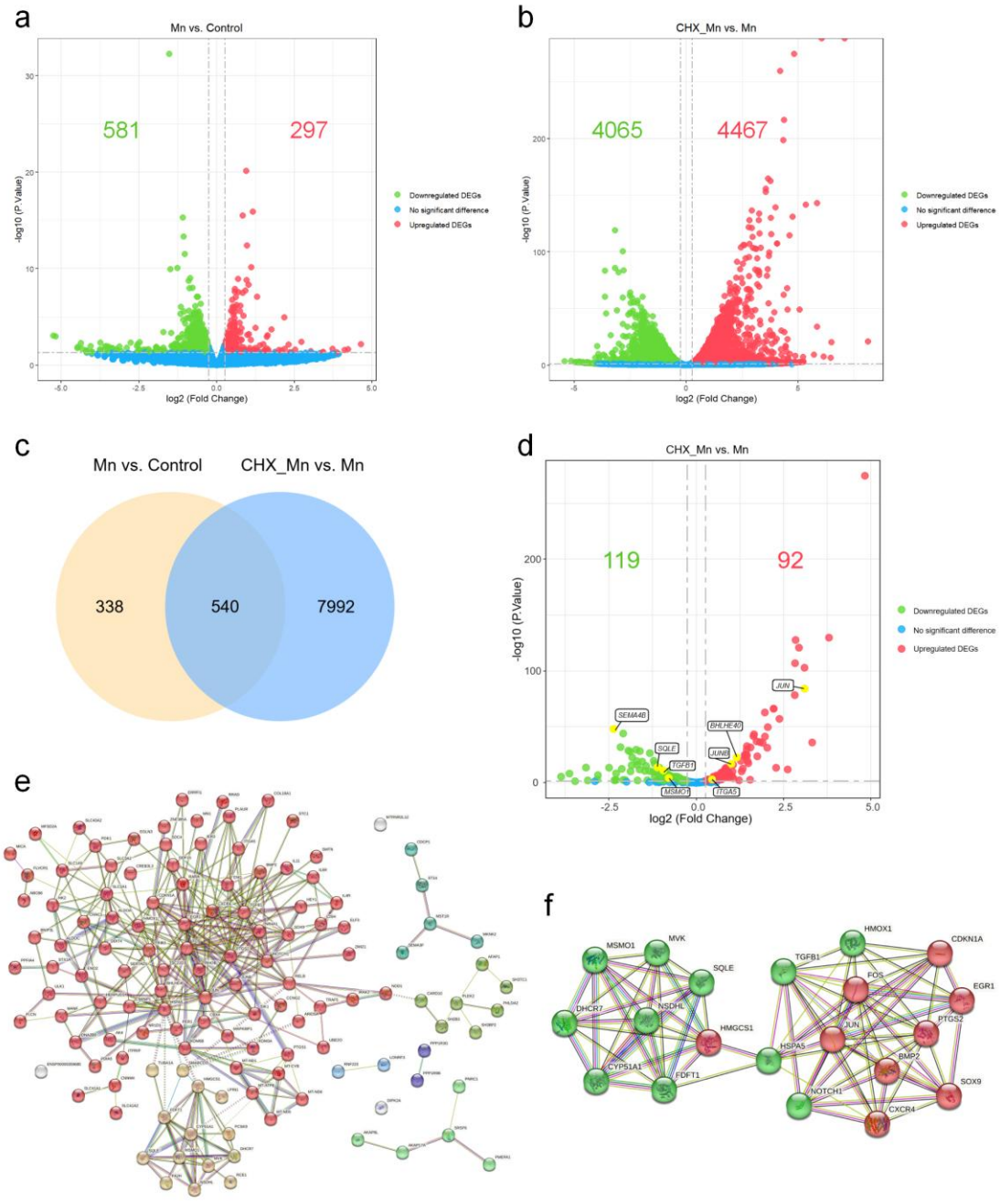


Fig. 3 Transcriptomic analysis and classification of Mn-induced PRGs and SRGs in A549 cells. After

A549 cells were treated with 300 μM $MnCl_2$ for 4 h and CHX were pretreated for 30 min before $MnCl_2$ treatment. RNA was extracted and transcriptomic assay was applied to analyze the DEGs. (a-b) The volcano plots display the gene expression in the Mn vs. Control group (a) and CHX_Mn vs. Mn group (b). Each point represents one of the detected genes. Green points are downregulated DEGs, red points are upregulated DEGs and blue points are genes without differential changes. Horizontal dotted lines indicate a $P<0.01$. (c) Summary of the numbers of overlapping DEGs between the Mn vs. Control group and CHX_Mn vs. Mn group. (d) The volcano plots display the gene expression of PRGs and SRGs. (e-f) The PPI Network (e) and the hub proteins network (f) of PRGs and SRGs. Each node represents a protein and the interaction between the two proteins is represented by a sideline connection. Different line colors represent different interactions. Mn: A549 cells were treated with 300 μM $MnCl_2$ for 4 h; CHX_Mn: A549 cells were treated with CHX 30 min before MnCl2 treatment; n=3

GO analysis of Mn-induced early response genes

The 92 classified PRGs and 119 classified SRGs were annotated with 662 and 717 GO annotations according to their biological processes, cellular components, and molecular functions. Sorted by *p*-value, the top 30 enriched GO terms were shown in Fig. 4. The PRGs and SRGs were annotated with 482 and 517 GO annotations according to their biological processes, respectively (Supplementary Table 3). Among these GO annotations, the PRGs and SRGs were enriched in 379 common GO annotations like response to oxygen levels, cellular response to external stimulus, response to oxidative stress, response to antibiotic and cellular response to drug. As for cellular components, the PRGs and SRGs were annotated with 68 and 81 GO annotations, respectively. With *p*-value <0.05 as the standard, they were both significantly enriched in 52 common GO annotations like receptor complex (GO:0043235). As for molecular functions, the PRGs and SRGs were annotated with 112 and 119 GO annotations,

respectively. They were enriched in 66 common GO annotations like chromatin DNA binding.

In addition, GO term of response to oxygen levels (GO: 0070482), which was significantly enriched in both PRGs and SRGs, was further investigated. There were 16 Mn-upregulated DEGs were involved in the GO term of response to oxygen levels. Among the Mn-upregulated DEGs, *STC1* had the highest change ($\log_2$ (Mn/C) = 1.31), followed by *EGR1* (1.02), *DDIT4* (0.97), *EGLN3* (0.89), *PTGS2* (0.87), *CDKN1A* (0.84), *PDK1* (0.69), *VEGFA* (0.68), *HMOX1* (0.62), *HK2* (0.60), *SLC2A1* (0.50), *CXCR4* (0.41), *TGFB1* (0.373), *BNIP3L* (0.367), *NOTCH1* (0.30), *BMP2* (0.29). Among these genes, *STC1*, *EGR1*, *PTGS2*, *CDKN1A*, *VEGFA*, *SLC2A1*, *CXCR4*, and *BMP2* were classified as be PRGs whereas *DDIT4*, *EGLN3*, *PDK1*, *HMOX1*, *HK2*, *TGFB1*, *BNIP3L*, and *NOTCH1* were classified as be SRGs. These indicated that Mn-responsive genes are primarily involved in oxygen levels.

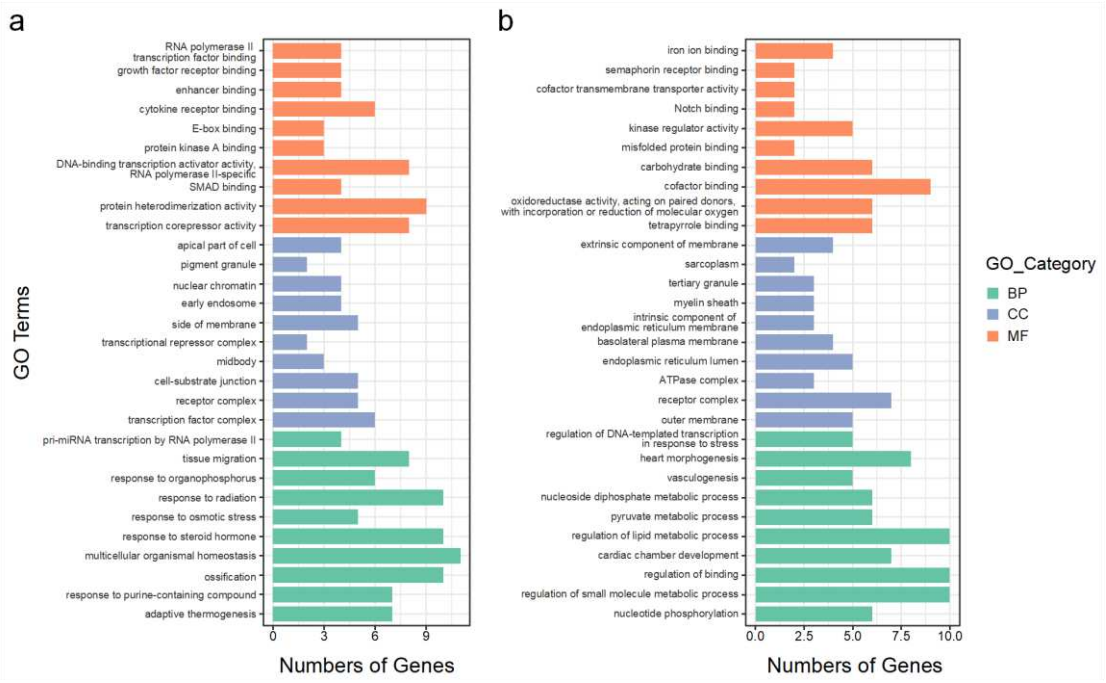


Fig. 4 GO analysis of Mn-induced early response genes. (a) GO enrichment histogram of PRGs. (b) GO enrichment histogram of SRGs. BP: biological process; CC: cellular component; MF: molecular functions

KEGG pathway analysis of Mn-induced early response genes

KEGG pathway analysis was performed with Mn-induced early response genes. The PRGs were annotated with 149 KEGG pathways whereas the SRGs included 152 KEGG pathways. The PRGs and SRGs were annotated with 99 common KEGG pathways. The top 20 enriched pathways were shown in Fig. 5. KEGG pathway analysis demonstrated that PRGs were most significantly enriched in the renal cell carcinoma (hsa05211), followed by circadian rhythm (hsa04710), rheumatoid arthritis (hsa05323), pathways in cancer (hsa05200) and HIF-1 signaling pathway (hsa04066). SRGs were most significantly enriched in the steroid biosynthesis (hsa00100), followed by HIF-1 signaling pathway (hsa04066), pathways in cancer (hsa05200), glycolysis/gluconeogenesis (hsa00010), and fructose and mannose metabolism (hsa00051) (Supplementary Table 4).

Furthermore, the most SRGs were annotated as the metabolic pathways (hsa01100) map identifiers, attaining 16 SRGs (*MVK*, *CHAC1*, *MSMO1*, *DHCR7*, *HK2*, *FDFT1*, *CYP51A1*, *ENO2*, *PTGS1*, *ALDOA*, *AK4*, *HMOX1*, *NSDHL*, *SQLE*, *LPIN1*, *ALDOC*), as well as 3 PRGs (*PTGS2*, *HMGCS1*, *DHRS3*). Note that both PRGs and SRGs played important roles in HIF-1 signaling pathway. There were 4 PRGs (*IL6R*, *VEGFA*, *CDKN1A*, *SLC2A1*) and 7 SRGs (*HK2*, *PDK1*, *MKNK2*, *ENO2*, *EGLN3*, *ALDOA*, *HMOX1*) annotated as the HIF-1 signaling pathway (hsa04066) map identifiers (Supplementary Fig. 1). These indicated the crucial role of HIF-1 signaling pathway in Mn exposure in A549 cells.

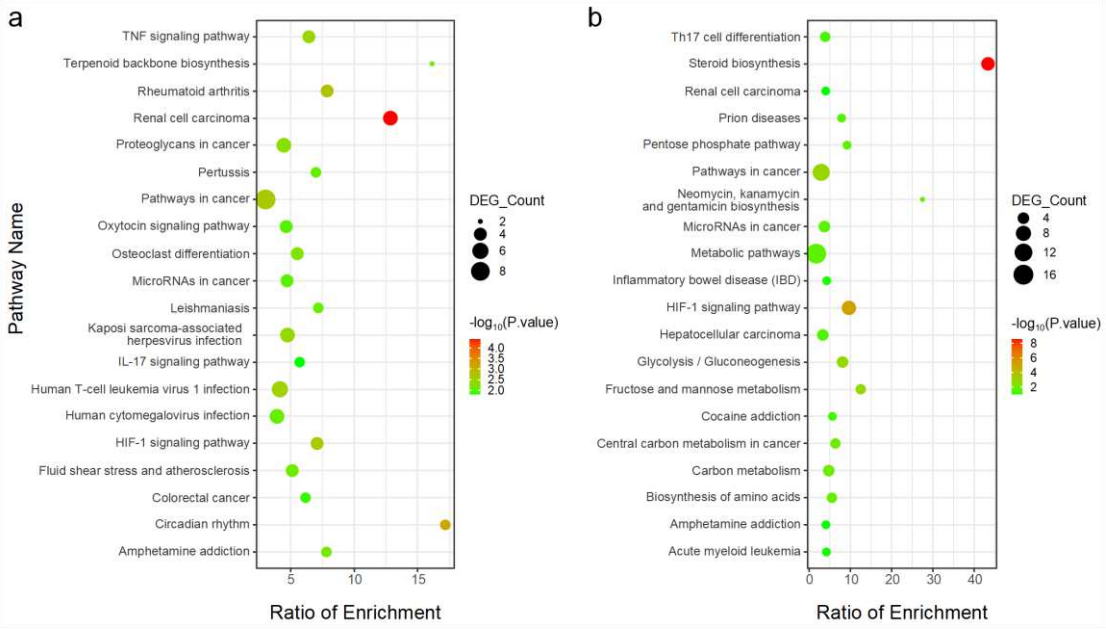


Fig. 5 KEGG analysis of Mn-induced early response genes. (a) KEGG pathway enrichment analysis of PRGs. (b) KEGG pathway enrichment analysis of SRGs. Rich factor indicates the ratio of annotated DEGs number and whole background genes number in the corresponding pathway. The size of each bubble corresponds to the number of annotated DEGs and the color gradient depicts the P value of enrichment significance

Experimental validation of PRGs and SRGs and dose-response characterization in Mn-induced A549 cells

After seeded in a 6-well plate for 12 h, the A549 cells were treated with 300 μM $MnCl_2$ for 4 h and 50 μM CHX were pretreated for 30 min before $MnCl_2$ treatment. RT-PCR was applied to analyze the effects of CHX on Mn-upregulated early response genes including *FOS*, *FOSB*, *JUN*, *JUNB*, *EGR1*, *PTGS2* and *HMOX1*. As shown in Fig. 6b, CHX pretreatment considerably increased the mRNA expression of *FOS*, *FOSB*, *JUN*, *JUNB*, *EGR1* and *PTGS2*, indicating that the induction of these genes is independent of de novo protein synthesis. Conversely, CHX pretreatment markedly suppressed the Mn-induced upregulation of *HMOX1*, suggesting that its expression requires prior protein synthesis. These findings

are consistent with the transcriptomic data and further support the classification of *FOS*, *FOSB*, *JUN*, *JUNB*, *EGR1* and *PTGS2* as PRGs while *HMOX1* serves as an SRG (Fig. 6c).

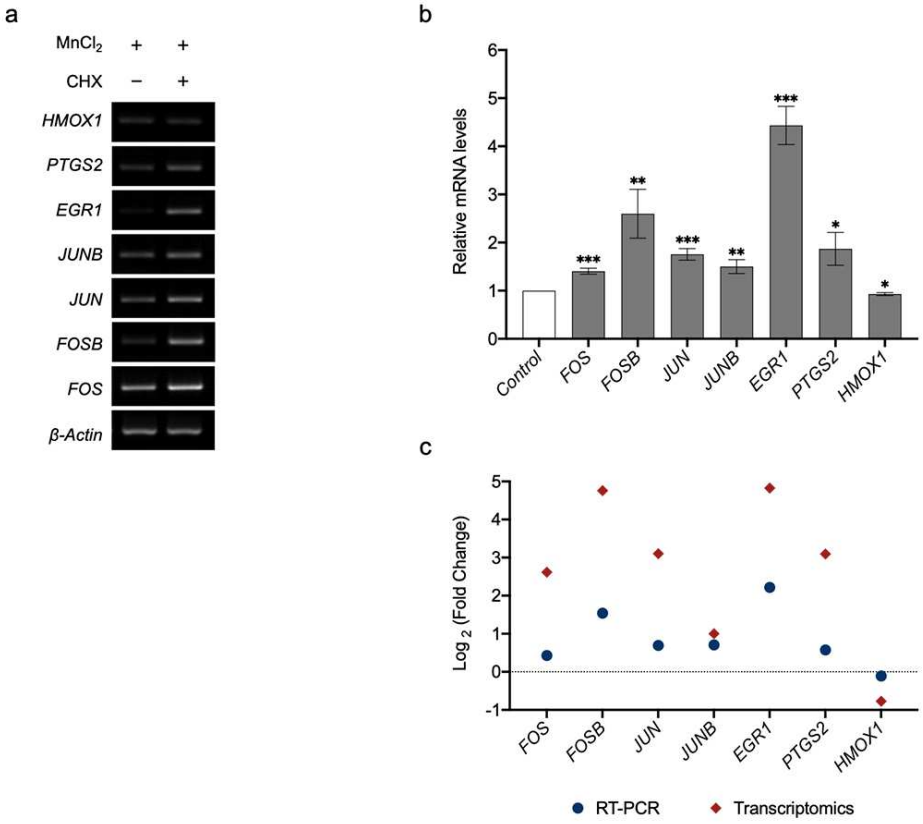


Fig. 6 Validation of CHX effects on Mn-upregulated early response genes in A549 cells. The A549 cells were treated with 300 μM $MnCl_2$ for 4 h and CHX were pretreated for 30 min before $MnCl_2$ treatment. (a) The density bands in RT-PCR. (b) The mRNA expression of early response genes was estimated by RT-PCR. (c) The comparative analysis of the effects of CHX on Mn-upregulated early response genes by RT-PCR and transcriptomic assay. The value was shown as mean ± SD, n = 3. Statistical significance was determined by a two-tailed paired Student's t test. *P < 0.05, **P < 0.01 and ***P < 0.005 (vs corresponding "Control" group)

Based on these results, RT-PCR was further applied to validate the transcriptomic classification of

significantly changed PRGs (*ITGA5*, *BHLHE40*, *VEGFA*, *CDKN1A*, *KDM3A*, *ARRDC3* and *IL11*) and SRGs (*SQLE*, *MSMO1*, *DHCR7*, *TGFB1* and *SEMA4B*). Building upon the robust transcriptional responses observed at 300 μM, we further expanded the dose-response investigation to a wider concentration gradient (0–1200 μM) over a short 4 h exposure. It is worth noting that cell viability assessments confirmed that this short-term (4 h) treatment across the entire 0–1200 μM range had no significant impact on cell proliferation and viability (data not shown). As shown in Fig.7 and Fig.8, the expression of most selected PRGs and SRGs increased significantly at 300 μM $MnCl_2$. However, beyond this concentration, the expression levels generally showed a dose-independent trend, with only minor fluctuations observed in a few genes.

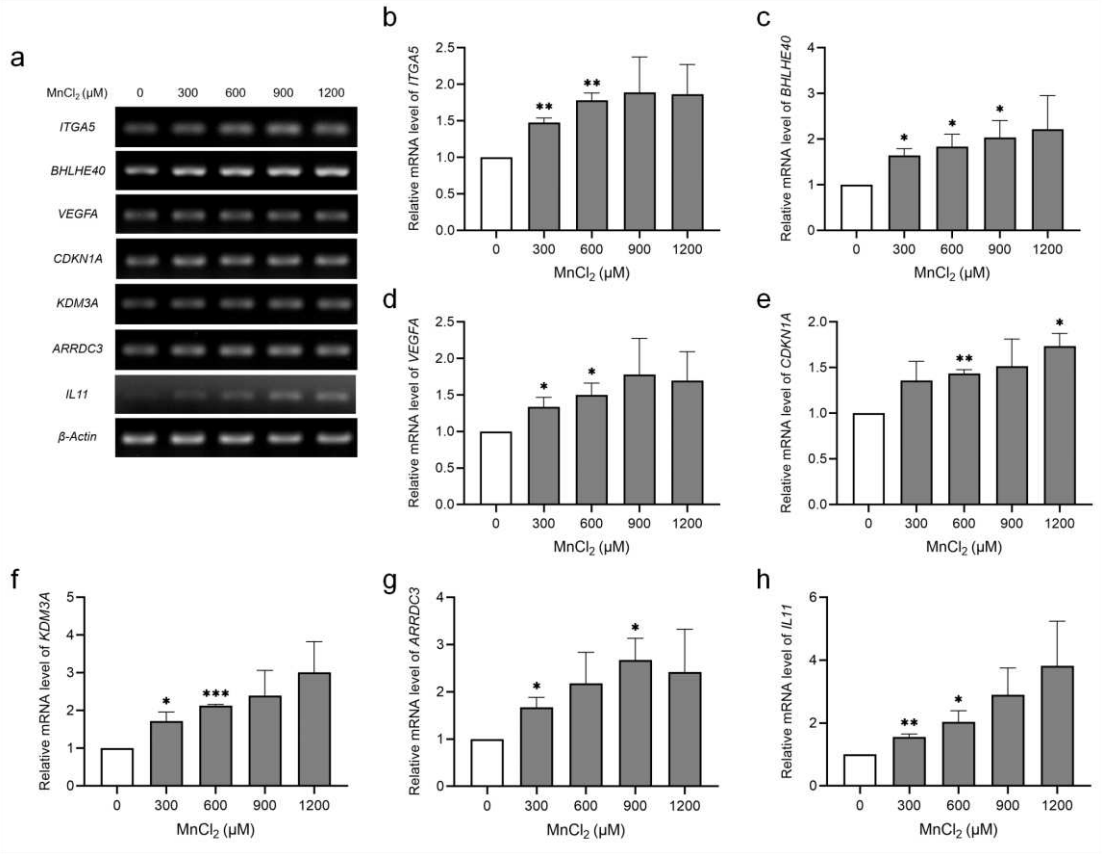


Fig. 7 Dose-response relationship of Mn-induced PRGs in A549 cells. The A549 cells were treated with 0-1200 μM $MnCl_2$ for 4 h. (a-h) The mRNA expression of PRGs was estimated by RT-PCR. The value

was shown as mean ± SD, n = 3. Statistical significance was determined by a two-tailed paired Student's t test. *P < 0.05, **P < 0.01 and ***P < 0.005 (vs corresponding "Mn" group)

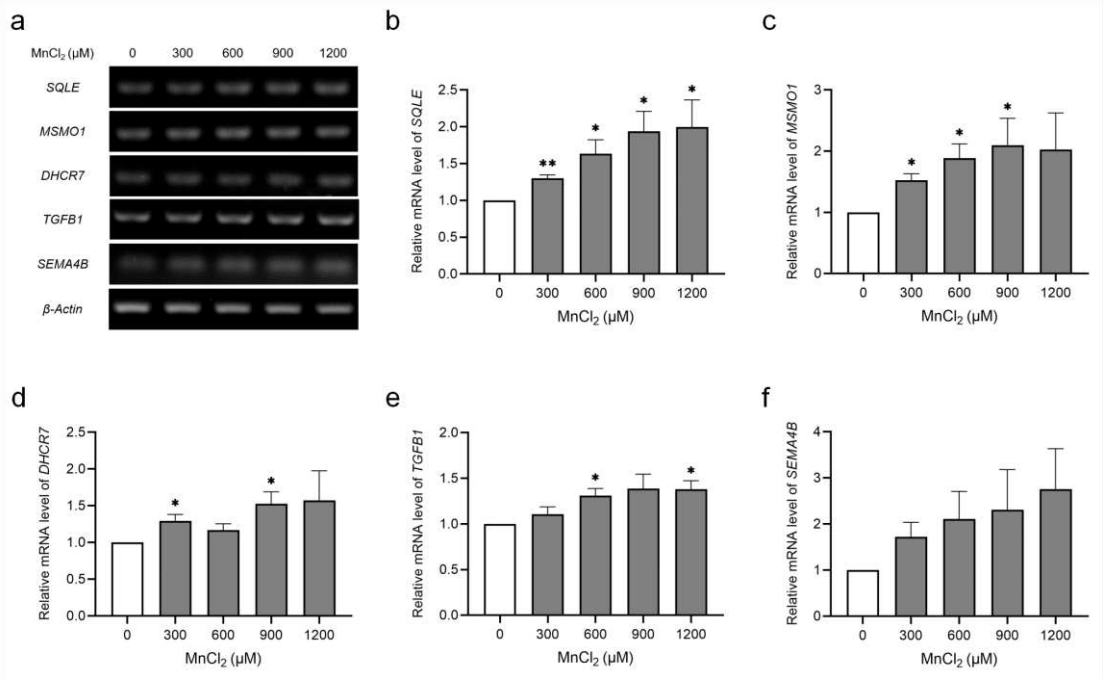


Fig. 8 Dose-response relationship of Mn-induced SRGs in A549 cells. The A549 cells were treated with 0-1200 μM $MnCl_2$ for 4 h. (a-f) The mRNA expression of SRGs was estimated by RT-PCR. The value was shown as mean ± SD, n = 3. Statistical significance was determined by a two-tailed paired Student's t test. *P < 0.05 and **P < 0.01 (vs corresponding "Mn" group)

To confirm their classification of PRGs and SRGs based on the requirement for de novo protein synthesis, we assessed the effect of CHX pretreatment under Mn exposure. As shown in Fig. 9, the mRNA expression of *ITGA5*, *BHLHE40*, *VEGFA*, *CDKN1A*, *KDM3A*, *ARRDC3* and *IL11* were upregulated following CHX treatment, regardless of Mn administration. This suggests that CHX itself may act as an external stimulus that transiently enhances the mRNA levels of these genes. These results confirm that their expression does not require de novo protein synthesis, a hallmark of PRGs. In contrast, CHX pretreatment significantly inhibited the Mn-induced upregulation of *SQLE*, *MSMO1*, *DHCR7*,

TGFB1 and *SEMA4B* (Fig. 10), aligning with the characteristics of SRGs. These results were highly consistent with the transcriptomic analysis. Taken together, *ITGA5*, *BHLHE40*, *VEGFA*, *CDKN1A*, *KDM3A*, *ARRDC3* and *IL11* were validated as PRGs, while *SQLE*, *MSMO1*, *DHCR7*, *TGFB1* and *SEMA4B* were confirmed as SRGs.

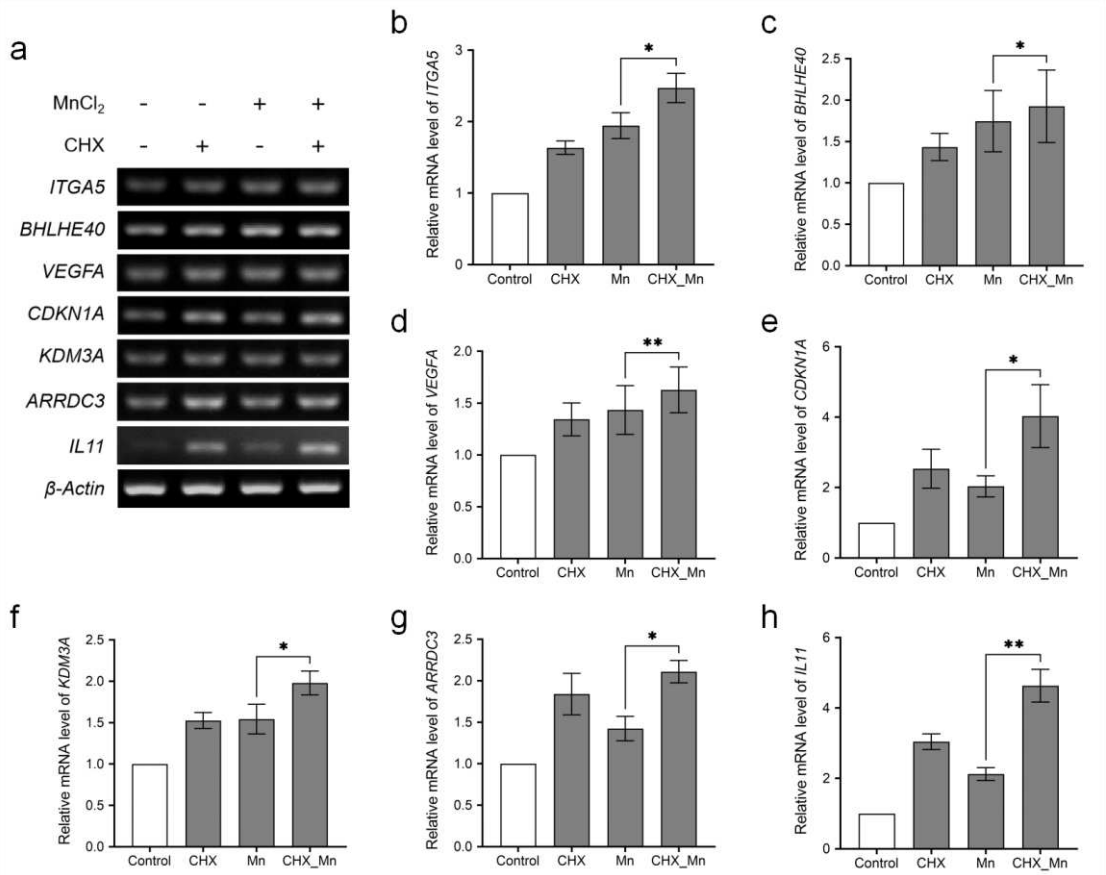


Fig. 9 Validation of PRG classification via CHX treatment in A549 cells. The A549 cells were treated with 300 μM $MnCl_2$ for 4 h and CHX were pretreated for 30 min before $MnCl_2$ treatment. (a-h) The mRNA expression of PRGs was estimated by RT-PCR. The value was shown as mean ± SD, n = 3. Statistical significance was determined by a two-tailed paired Student's t test. *P < 0.05 and **P < 0.01 (vs corresponding "Mn" group)

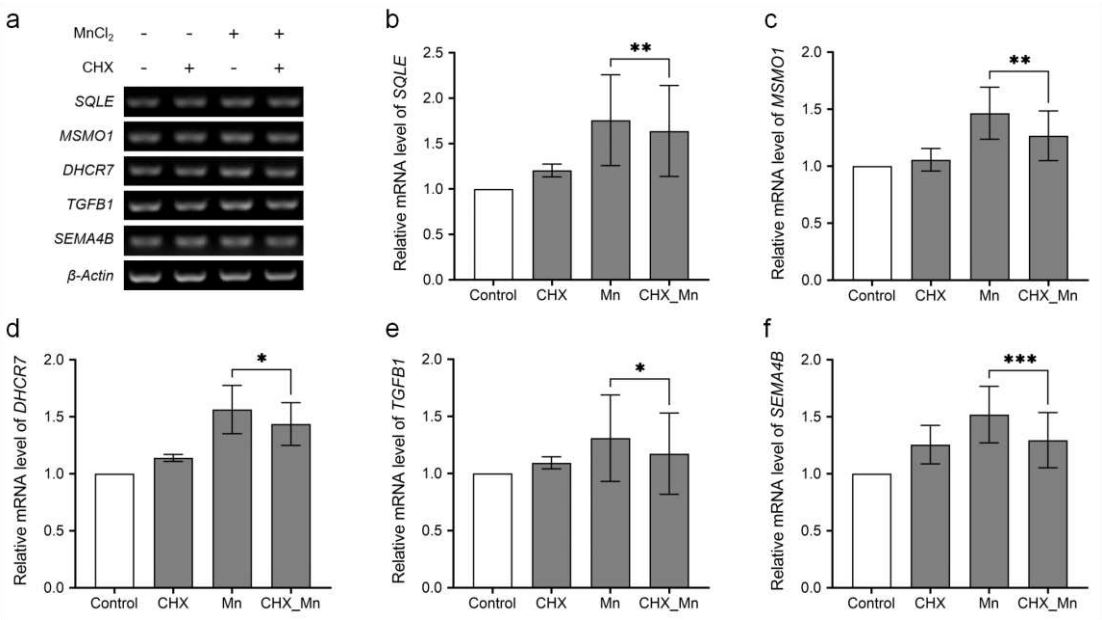


Fig. 10 Validation of SRG classification via CHX treatment in A549 cells. The A549 cells were treated with 300 μM $MnCl_2$ for 4 h and CHX were pretreated for 30 min before $MnCl_2$ treatment. (a-f) The mRNA expression of SRGs was estimated by RT-PCR. The value was shown as mean ± SD, n = 3. Statistical significance was determined by a two-tailed paired Student's t test. *P < 0.05, **P < 0.01 and ***P < 0.005 (vs corresponding "Mn" group)

Discussion

In this study, we systematically integrated genome-wide transcriptomics with RT-PCR validation to identify Mn-induced early response genes. We successfully classified 92 PRGs and 119 SRGs induced by a sub-lethal 300 μM Mn dose. This dose selection is crucial: while physiological serum Mn is trace, occupational exposures (e.g., in mining, welding, and battery manufacturing) result in localized pulmonary accumulations that far exceed circulating levels. Our dose-response data (Fig. 7, 8) demonstrated that while lower, physiologically adjacent doses (10-100 μM) initiated minor transcriptional shifts, the 300 μM concentration was required to robustly activate the cellular stress signaling cascade without plunging the A549 cells into immediate necrosis, thus providing a clear

window into early toxicity mechanisms.

Our temporal analysis corroborated that *FOS*, *FOSB*, *JUN*, *JUNB*, *EGR1*, and *PTGS2* behave as classical immediate-early PRGs. The prominent induction of AP-1 complex members (*JUN/FOS*) underscores their pivotal role as "first responders" to Mn insult. Utilizing CHX pretreatment allowed us to definitively separate primary signaling from secondary cascades [29,30]. Interestingly, several PRGs (e.g., *FOS*, *JUN*, *EGR1*) exhibited "superinduction" when treated with CHX. This phenomenon occurs because blocking translation prevents the synthesis of labile repressor proteins that normally shut down PRG transcription, thereby stabilizing and amplifying the PRG mRNA transcripts [31,32]. Our RT-PCR validation carefully accounted for this, confirming that while CHX itself can be a stressor, the defining feature of PRGs—their independence from de novo translation—holds true for our identified Mn-responsive targets.

Unlike previous studies focusing on single oxidative stress markers, our transcriptomic approach reveals that the number of identified Mn-induced PRGs (92) is highly comparable to SRGs (119), demonstrating a massive, coordinated initial genomic shift. This broad transcriptional remodeling mirrors the complex stress and unfolded protein responses recently observed in in vivo transcriptomic models of Mn toxicity [33]. The protein-protein interaction network confirms that PRGs serve as highly connected regulatory hubs initiating downstream SRG cascades [34].

A major finding of this study is the bioinformatic convergence of both PRGs and SRGs on "response to oxygen levels" and the HIF-1 signaling pathway. Although Mn is classically known to induce ROS and mitochondrial dysfunction [19], its direct intersection with hypoxia-like signaling in lung epithelium is profound. HIF-1 acts as a master transcriptional regulator under hypoxic stress, profoundly altering cellular metabolism [35]. Recent literature indicates that elevated Mn directly

stabilizes HIF-1α and HIF-2α to upregulate specific transporters (like *SLC30A10*) as a homeostatic defense mechanism against Mn toxicity [36]. Our data show that Mn exposure acutely triggers a phased HIF-1-related response, beginning with PRGs like *VEGFA* and *CDKN1A*, and subsequently activating metabolic SRGs like *HK2* and *HMOX1*. *HMOX1* is a critical antioxidant gene whose delayed induction (SRG) aligns with its role in managing downstream heme/iron-related oxidative stress [37,38].

While this study establishes a robust transcriptional classification of Mn toxicity, it is not without limitations. Although our transcriptomic and RT-PCR data are strongly concordant, functional protein-level validations are necessary to fully substantiate the functional execution of these pathways. Future studies employing specific HIF-1 inhibitors or in vivo inhalation models will be critical to determine whether targeting this early PRG-SRG cascade can therapeutically mitigate Mn-induced respiratory damage.

Conclusion

This study provides a comprehensive mapping of the immediate-early transcriptomic architecture triggered by acute manganese exposure in lung epithelial cells. Rather than focusing solely on end-point cytotoxicity, we successfully identified and mechanistically classified the initial wave of 92 PRGs (e.g., *FOS*, *JUN*, *EGR1*) and the subsequent 119 SRGs (e.g., *HMOX1*, *SQLE*). Our integrated bioinformatic and experimental approach highlights that Mn toxicity rapidly activates oxygen-sensing networks and the HIF-1 signaling pathway, driving early metabolic and oxidative stress responses. These findings shift the paradigm of Mn toxicity from generic oxidative damage to a highly regulated, phased transcriptional cascade, offering novel early-response biomarkers and identifying the HIF-1 axis as a potential target for the prevention of occupational lung injury.

References

1. Yokel RA (2009) Manganese flux across the blood-brain barrier. Neuromolecular Med 11:297-310. https://doi.org/10.1007/s12017-009-8101-2
2. Chen P, Bornhorst J, Aschner M (2018) Manganese metabolism in humans. Front Biosci (Landmark Ed) 23:1655-1679. https://doi.org/10.2741/4665
3. Rahman SM, Kippler M, Tofail F, Bolte S, Hamadani JD, Vahter M (2017) Manganese in Drinking Water and Cognitive Abilities and Behavior at 10 Years of Age: A Prospective Cohort Study. Environ Health Perspect 125:057003. https://doi.org/10.1289/EHP631
4. Myers JE, teWaterNaude J, Fourie M, Abie Zogoe HB, Naik I, Theodorou P et al (2003) Nervous system effects of occupational manganese exposure on South African manganese mineworkers. Neurotoxicology 24:649-656. https://doi.org/10.1016/S0161-813X(03)00035-4
5. Zaitseva NV, Zemlyanova MA, Gekht AB, Dedaev SI, Kol'dibekova YV, Peskova EV et al (2025) Neurotoxic effects of aluminum and manganese: From molecular to clinical effects. J Neurol Sci 473:123480. https://doi.org/10.1016/j.jns.2025.123480
6. Guilarte TR (2010) Manganese and Parkinson's disease: a critical review and new findings. Environ Health Perspect 118:1071-1080. https://doi.org/10.1289/ehp.0901748
7. Gandhi D, Rudrashetti AP, Rajasekaran S (2022) The Impact of Environmental and Occupational Exposures of Manganese on Pulmonary, Hepatic, and Renal Functions. J Appl Toxicol 42:103-129. https://doi.org/10.1002/jat.4214
8. Fan NC, Huang HY, Wang SL, Tseng YL, Chang-Chien J, Tsai HJ et al (2023) Association of exposure to environmental vanadium and manganese with lung function among young children: A population-based study. Ecotoxicol Environ Saf 264:115430. https://doi.org/10.1016/j.ecoenv.2023.115430
9. Cirelli C, Pompeiano M, Tononi G (1995) In vivo antisense approaches to the role of immediate early gene expression in the brain. Regul Pept 59:151-162. https://doi.org/10.1016/0167-0115(95)00097-u
10. Lau LF, Nathans D (1987) Expression of a set of growth-related immediate early genes in BALB/c 3T3 cells: coordinate regulation with c-fos or c-myc. Proc Natl Acad Sci U S A 84:1182-1186. https://doi.org/10.1073/pnas.84.5.1182
11. Bahrami S, Drablos F (2016) Gene regulation in the immediate-early response process. Adv Biol Regul 62:37-49. https://doi.org/10.1016/j.jbior.2016.05.001
12. Healy S, Khan P, Davie JR (2013) Immediate early response genes and cell transformation. Pharmacol Ther 137:64-77. https://doi.org/10.1016/j.pharmthera.2012.09.001
13. Boldogh I, AbuBakar S, Albrecht T (1990) Activation of proto-oncogenes: an immediate early event in human cytomegalovirus infection. Science 247:561-564. https://doi.org/10.1126/science.1689075
14. 14. Herschman HR (1991) Primary response genes induced by growth factors and tumor promoters. Annu Rev Biochem 60:281-319. https://doi.org/10.1146/annurev.bi.60.070191.001433
15. 15. Hughes P, Dragunow M (1995) Induction of immediate-early genes and the control of neurotransmitter-regulated gene expression within the nervous system. Pharmacol Rev 47:133-178. https://doi.org/10.1016/S0031-6997(25)06819-X
16. 16. Fowler T, Sen R, Roy AL (2011) Regulation of primary response genes. Mol Cell 44:348-360. https://doi.org/10.1016/j.molcel.2011.09.014

17. 17. Shan Y, Carlock LR, Walker PD (1997) NMDA receptor overstimulation triggers a prolonged wave of immediate early gene expression: relationship to excitotoxicity. Exp Neurol 144:406-415. https://doi.org/10.1006/exnr.1997.6427
18. 18. Walker PD, Carlock LR (1993) Immediate early gene activation during the initial phases of the excitotoxic cascade. J Neurosci Res 36:588-595. https://doi.org/10.1002/jnr.490360511
19. 19. Johnston LJ, Du X, Zborowski A, Kennedy DC (2024) Characterization and Cellular Toxicity Studies of Commercial Manganese Oxide Nanoparticles. Nanomaterials (Basel) 14:198. https://doi.org/10.3390/nano14020198
20. 20. Xia L, Park JH, Biggs K, Lee CG, Liao L, Shannahan JH (2023) Compositional variations in metal nanoparticle components of welding fumes impact lung epithelial cell toxicity. J Toxicol Environ Health A 86:735-757. https://doi.org/10.1080/15287394.2023.2238209
21. 21. Setkov NA, Kazakov VN, Rosenwald IB, Makarova GF, Epifanova OI (1992) Protein synthesis inhibitors, like growth factors, may render resting 3T3 cells competent for DNA synthesis: a radioautographic and cell fusion study. Cell Prolif 25:181-191. https://doi.org/10.1111/j.1365-2184.1992.tb01393.x
22. 22. Müller R, Bravo R, Burckhardt J, Curran T (1984) Induction of c-fos gene and protein by growth factors precedes activation of c-myc. Nature 312:716-720. https://doi.org/10.1038/312716a0
23. 23. Díaz C, López F, Henríquez P, Rodríguez E, Serra-MaJem L (2001) Serum manganese concentrations in a representative sample of the Canarian population. Biol Trace Elem Res 80:43-51. https://doi.org/10.1385/BTER:80:1:43
24. 24. Gao F, Kataoka M, Liu N, Liang T, Huang ZP, Gu F et al (2019) Therapeutic role of miR-19a/19b in cardiac regeneration and protection from myocardial infarction. Nat Commun 10:1802. https://doi.org/10.1038/s41467-019-09530-1
25. 25. Liao Y, Wang J, Jaehnig EJ, Shi Z, Zhang B (2019) WebGestalt 2019: gene set analysis toolkit with revamped UIs and APIs. Nucleic Acids Res 47:W199-W205. https://doi.org/10.1093/nar/gkz401
26. 26. Kanehisa M, Goto S (2000) KEGG: Kyoto encyclopedia of genes and genomes. Nucleic Acids Res 28:27-30. https://doi.org/10.1093/nar/28.1.27
27. 27. Milde-Langosch K (2005) The Fos family of transcription factors and their role in tumourigenesis. Eur J Cancer 41:2449-2461. https://doi.org/10.1016/j.ejca.2005.08.008
28. 28. Zenz R, Wagner EF (2006) Jun signalling in the epidermis: From developmental defects to psoriasis and skin tumors. Int J Biochem Cell Biol 38:1043-1049. https://doi.org/10.1016/j.biocel.2005.11.011
29. 29. Allinson ET, Drucker DJ (1992) Parathyroid hormone-like peptide shares features with members of the early response gene family: rapid induction by serum, growth factors, and cycloheximide. Cancer Res 52:3103-3109.
30. 30. Lusska A, Wu L, Whitlock JP Jr (1992) Superinduction of CYP1A1 transcription by cycloheximide. Role of the DNA binding site for the liganded Ah receptor. J Biol Chem 267:15146-15151. https://doi.org/10.1016/S0021-9258(18)42158-8
31. 31. Greenberg ME, Hermanowski AL, Ziff EB (1986) Effect of protein synthesis inhibitors on growth factor activation of c-fos, c-myc, and actin gene transcription. Mol Cell Biol 6:1050-1057. https://doi.org/10.1128/mcb.6.4.1050-1057.1986

32. 32. Megyesi J, Di Mari J, Udvarhelyi N, Price PM, Safirstein R (1995) DNA synthesis is dissociated from the immediate-early gene response in the post-ischemic kidney. Kidney Int 48:1451-1458. https://doi.org/10.1038/ki.1995.434
33. 33. Nicolai MM, Pirritano M, Gasparoni G, Aschner M, Simon M, Bornhorst J (2022) Manganese-Induced Toxicity in *C. elegans*: What Can We Learn from the Transcriptome? Int J Mol Sci 23:10748. https://doi.org/10.3390/ijms231810748
34. 34. Tullai JW, Schaffer ME, Mullenbrock S, Sholder G, Kasif S, Cooper GM (2007) Immediate-early and delayed primary response genes are distinct in function and genomic architecture. J Biol Chem 282:23981-23995. https://doi.org/10.1074/jbc.M702044200
35. 35. Denko NC (2008) Hypoxia, HIF1 and glucose metabolism in the solid tumour. Nat Rev Cancer 8:705-713. https://doi.org/10.1038/nrc2468
36. 36. Liu C, Jursa T, Aschner M, Smith DR, Mukhopadhyay S (2021) Up-regulation of the manganese transporter SLC30A10 by hypoxia-inducible factors defines a homeostatic response to manganese toxicity. Proc Natl Acad Sci U S A 118:e2107673118. https://doi.org/10.1073/pnas.2107673118
37. 37. Otterbein LE, Soares MP, Yamashita K, Bach FH (2003) Heme oxygenase-1: unleashing the protective properties of heme. Trends Immunol 24:449-455. https://doi.org/10.1016/s1471-4906(03)00181-9
38. 38. Yang G, Nguyen X, Ou J, Rekulapelli P, Stevenson DK, Dennery PA (2001) Unique effects of zinc protoporphyrin on HO-1 induction and apoptosis. Blood 97:1306-1313. https://doi.org/10.1182/blood.v97.5.1306

Statements and Declarations

Funding

This work was supported by grants from National Natural Science Foundation of China (No. 81573192), Scientific and Technological Innovation Project of China Academy of Chinese Medical Sciences (No. CI2023C020YL) and the Fundamental Research Funds for the Central Universities (No. JK2024-2-07).

Competing interests

Financial interests: The authors declare that they have no known competing financial interests or personal relationships that could have appeared to influence the work reported in this paper.

Author Contributions

Xinyu Liu: Data curation, Software, Supervision, Validation, Visualization, Writing - original draft. **Yishan Jin:** Data curation, Methodology, Resources, Software, Validation. **Shuiqing Yang:** Conceptualization, Data curation, Formal analysis, Investigation, Methodology, Software, Validation, Visualization. **Huizhi Xiang:** Software, Visualization. **Chunhong Yu:** Conceptualization, Data curation, Formal analysis, Funding acquisition, Investigation, Methodology, Project administration, Supervision, Writing - original draft, Writing - review & editing. **Zongchun Yi:** Conceptualization, Funding acquisition, Investigation, Methodology, Project administration, Writing - review & editing. All authors read and approved the final manuscript.

Data availability

The datasets of the current study are available from the corresponding author upon reasonable request.

Ethics approval

The manuscript does not contain clinical studies or patient data.

Supplementary Files

This is a list of supplementary files associated with this preprint. Click to download.

- SupplementaryInformations.pdf